First results from the PADME experiment - getting ready for dark sector studies

Isabella Oceano on behalf of PADME collaboration [d].
Dipartimento di matematica e fisica, Università del Salento,
Lecce,Italy

Dark Sector searches are nowadays an anchor asset of many particle physics experiments at accelerators. The Positron Annihilation into Dark Matter Experiment (PADME), ongoing at the Laboratori Nazionali di Frascati of INFN, is looking for hidden particle signals by studying the missing mass spectrum of single-photon final states resulting from positrons annihilation with electrons of a fixed target. PADME collected during RUN II data taking in 2020 a sample of 6×10^{12} positron on target collisions. From a subset of the RUN II data sample, the cross-section of the process $e^+e^- \to \gamma\gamma$ has been measured with 5% precision at $\sqrt{s} = 21$ MeV. This represents the most precise measurement of the $e^+e^- \to \gamma\gamma$ cross section below 1 GeV. The preliminary result of this study is presented for the first time, and it is compared with theoretical QED expectations at Next to Leading Order.

1 Introduction

The Standard Model (SM) of particle physics is a quantum field theory that describes the behaviour of fundamental particles interacting through the strong, electromagnetic and weak forces with extreme accuracy. Although the SM has an extraordinary record of successes, it still fails to explain some of the more prominent physical phenomena observed in the universe. An ever-increasing amount of evidence suggests that most of the universe's content is composed of some non-luminous, hitherto unknown, "Dark Matter" (DM). The best motivated DM candidates are the WIMP (Weak Interacting Massive Particles), massive particles ($\sim 10^2$ GeV), interacting weakly with the known matter. Despite the enthusiasm for these new particles hypothesis, severe constraints were put on these models . This motivates the investigation of other dark matter candidate hypotheses. A possible alternative model consists in the introduction of a new hidden sector with a new Abelian gauge symmetry $U_D(1)$ besides the SM symmetry. As a consequence, a new massive gauge boson A', called dark photon, is predicted. The interaction between the SM fermions and the new gauge field can happen via "kinetic mixing" with SM photon through the Lagrangian term $L_{int} = \frac{\epsilon}{2} F^{\mu\nu}_{QED} F^{Dark}_{\mu\nu}$, where ϵ is the the kinetic mixing coefficient. This may be so small ($\sim 10^{-3}$) to have precluded so far the experimental discovery of the dark photon.

[d] A.P. Caricato, M. Martino, I. Oceano, S. Spagnolo (INFN Lecce and Salento Univ.), G. Chiodini (INFN Lecce), F. Bossi, R. De Sangro, C. Di Giulio, D. Domenici, G. Finocchiaro, L.G. Foggetta, M. Garattini, A. Ghigo, P. Gianotti, I. Sarra, T. Spadaro, E. Spiriti, C. Taruggi, E. Vilucchi (INFN Laboratori Nazionali di Frascati), V. Kozhuharov (So a Univ. "St. Kl. Ohridski" and INFN Laboratori Nazionali di Frascati), S. Ivanov, Sv. Ivanov, R. Simeonov (So a Univ. "St. Kl. Ohridski"), G. Georgiev (So a Univ. "St. Kl. Ohridski" and INRNE Bulgarian Academy of Science), F. Ferrarotto, E. Leonardi, P. Valente, A. Variola (INFN Roma1), E. Long, G.C. Organtini, G. Piperno, M. Raggi (INFN Roma1 and "Sapienza" Univ. Roma), S. Fiore (ENEA Frascati and INFN Roma1), V. Capirossi, F. Iazzi, F. Pinna (Politecnico of Torino and INFN Torino), A. Frankenthal (Princeton University)

A variety of dark photon production mechanisms have been exploited in dark photon searches: A'-strahlung on nuclei $e^{\pm}N \to e^{\pm}NA'$, annihilation process $e^+e^- \to \gamma A'$, neutral meson decays like π^0, η, ϕ and Υ and the Drell-Yan (DY) $q\bar{q} \to A' \to l^+l^-, h^+h^-$. According to the mass hierarchy of the dark sector, the A' decay phenomenology can occur with two scenarios. The dark photon will decay in SM particles with a $\Gamma \propto \epsilon^2$ if $2m_\chi > m_{A'}$, where χ is a DM particle; otherwise if $m_{A'} > 2m_\chi$, the main decay mode will be $A' \to \chi\chi$, since it is not suppressed by the ϵ factor. Considering these decay modes, the A' search can be classified in visible and invisible searches.

2 The PADME experiment

PADME is an experiment taking place at the Laboratori Nazionali di Frascati (LNF) of INFN designed to probe the dark photon hypothesis in the invisible decay mode. The A' production occurs via the annihilation process $e^+e^- \to \gamma A'$ and the strategy for its identification is to search for a peak in the missing mass $M^2_{miss} = (\vec{p_{e^+}} + \vec{p_{e^-}} \quad \vec{p_\gamma})^2$ distribution.

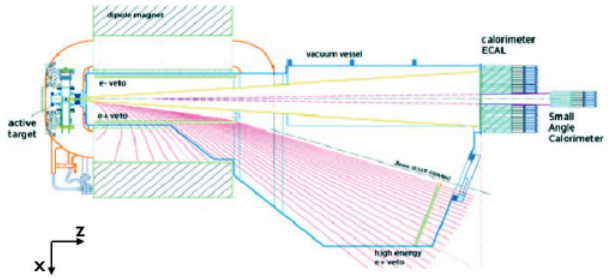

Figure 1: Layout of the PADME experiment (top view).

PADME was approved by INFN in 2016 and installed in 2018 at the LNF[2]. The LINAC of DAΦNE [3] provides a positron beam with $E_{e^+} \leq 550$ MeV. Since the production happens via positron-electron annihilation, the maximum value allowed of $m_{A'}$ at PADME is $m_{A'} = 23.7$ MeV. Figure 1 shows a layout of the experiment, entering from the left, the beam hits an active CVD Diamond target [4], and then propagates inside a vacuum chamber placed in the gap of a magnetic dipole. The neutral particles produced in the target, reach an electromagnetic calorimeter system placed in the forward direction, consisting of the main calorimeter (ECAL) [5] and of the Small Angle Calorimeter (SAC) [6]. The ECAL consists of 616 BGO crystals arranged in a cylindrical matrix with a 5×5 cm^2 central squared hole. Its main purpose is to detect the ordinary photons produced in association with the A'. The SAC is installed behind the central hole of ECAL calorimeter. It consists of a 5×5 matrix of PbF_2 Cherenkov crystals and provides fast detection and rejection of forward photons produced by Bremsstrahlung of the positron beam on the target. The detection of charged particles is performed by means of a veto system. It is located inside the PADME vacuum vessel and consists of three stations of plastics scintillators (EVeto for e^-, PVeto for e^+ and HEPVeto for high energy e^+) [7].

The installation of the PADME detector began in July 2018, and already on September 15th, the experiment started taking data. The experiment collected data for a commissioning run, called Run I, from November 2018 to March 2019. Run I allowed to understand the unexpected beam background, its sources and how to reduced it [8]. The Run II data were collected with improved beam parameters and beam-line configuration. From September to December 2020 a total integrated luminosity of $L_{RunII} = (5.47 \pm 0.27) \times 10^{\ 2}$ POT was collected.

3 $e^+e^- \to \gamma\gamma$ cross-section

The two-photon annihilation is a precious SM process for PADME. The study of this process allows to monitor the apparatus energy scale, to measure independently the number of positrons hitting the target, to cross-check the detector geometry and to determine the beam direction and position. In addition, it allows to set-up an efficient background rejection strategy for the dark photon search. The signature of this process consists in the presence of two photons in the electromagnetic calorimeters. The two-photon annihilation cross-section measurement

presented in this paper was performed for a beam energy $E_{beam} = 430$ MeV using 4×10 POT approximately 10% of the Run II data set.

The data selection exploits the constrained di-photon kinematics. The sum of the two photon energies is equal to the beam energy $E + E_2 = E_{beam}$, and their transverse momenta are back to back, $\phi + \pi = \phi_2$. In addition, the energy E_i is a function of the radial position R_i as shown in Figure 2 (a), this is equivalent to assert that the energy is a function of the polar angle $E = f(R(\theta))$. As a consequence of the energy conservation and of the energy-polar angle dependence, θ and θ_2 are strictly correlated. Knowing the energy E of a photon sets its polar angle θ and the energy E_2 and the polar angle θ_2 of the second photon. Similarly, knowing the azimuthal angles ϕ of a photon sets the azimuthal angles ϕ_2 of the other.

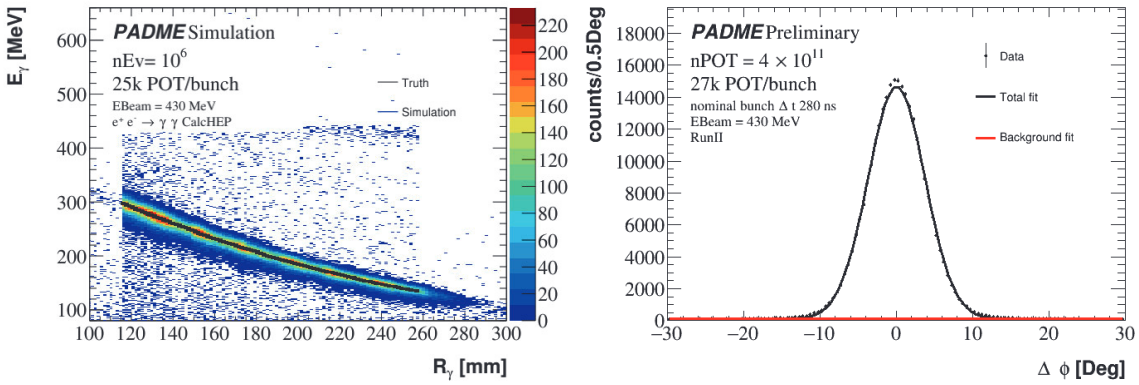

Figure 2: (a) Correlation between energy and radial position of photons in two-photon annihilation events generated by CalcHEP and reconstructed in PADME with pileup events. (b) $\Delta\phi$ distribution for two-photon selection in data (points), t curve (black line) and background component of the t (red line).

The selection of two-photon annihilation events is based on the search of two good quality photons[a] in time within 10 ns, with an energy above a given threshold ($E_\gamma > 90$ MeV) and with an energy and radial position compatible with the constrained kinematic $|\Delta E| = |E_\gamma \quad f(R_\gamma)| <$ 100 MeV. To reject photons reconstructed from clusters a ected by transverse energy leakage problems, a Fiducial Region (FR) is defined. The minimum radius for the most energetic photon implies a maximum radius for the other and vice-versa. The FR (115.8 mm $< R_\gamma <$ 250 mm) was chosen simulating the calorimeter response for two and three photons annihilation events generated with Babayaga [9] at NLO. With the same simulated sample, the acceptance of the process in this FR was determined to be $A = 0.06424 \pm 0.00025$. The two-photon annihilation yield was measured fitting the distribution $\Delta\phi = \phi + \pi \quad \pi_2$, which has an almost flat background. Figure 2 (b) shows the $\Delta\phi$ distribution with superimposed a fit function given by a second order polynomial and a Gaussian. The signal yield is measured by integrating the di erence between the distribution and the background component given by the polynomial part of the fit. The resulting yields was 276700 ± 530 where the error is statistical only.

An ad-hoc tag-and-probe technique was developed to measure the photon selection efficiency for two-photon annihilation events. Each good quality photon satisfies the requirement $|\Delta E| <$ 100 MeV defining a tag and a probe hypothesis exploiting the constrained annihilation kinematic. The distribution of the tags for one of the 8 inner azimuthal bins, is shown in Figure 3 (a), where the fit curve and its components are superimposed: two Gaussian functions for the signal, a beam background template, obtained from data with target out, and the pileup template, obtained from MC simulation. For each tag the search for a good quality photon that matches the probe hypothesis was done requiring $E > 90$ MeV, $|\Delta E| < 100$ MeV, in time within 7 ns and back-to-back within 45°. The photons passing this selection and within 3σ from

[a] The de nition of a good quality photon is based on the topology of the reconstructed clusters.

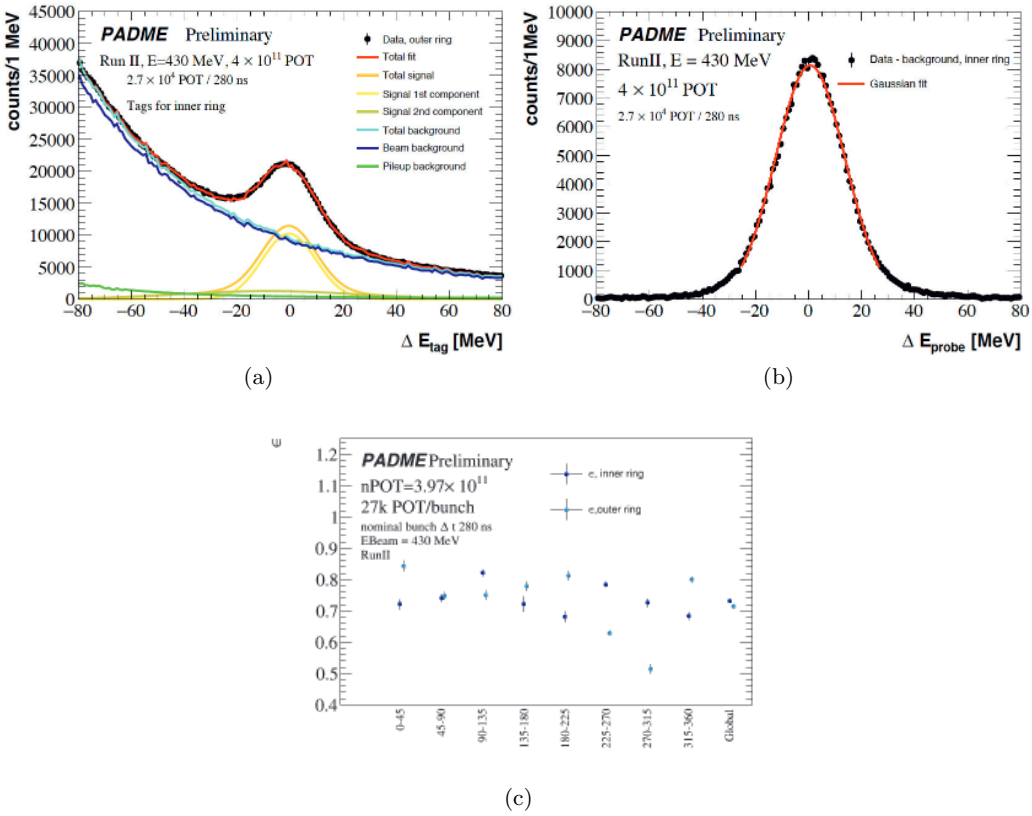

Figure 3: (a) Data (points) and t (red curve) of the ΔE_{Tag} distribution for tag photons in the inner ring of ECAL. The components of the total t function are shown separately: a total signal component in orange (sum of two Gaussian functions in light and acid yellow) and a total background component in cyan (sum of the pileup component, in green, and the beam related background, in blue). (b) Data (points) of the ΔE_{probe} distribution for matched probe photons with superimposed the Gaussian part of the t. (c) Photon selection efficiency for different bins.

the peak of $\Delta E_{probe} = E_{probe} + f(\theta_{tag})$ E_{Beam}, where $E_{beam} = 430$ MeV, were counted as matched probe. Once subtracted of the background, the tag-and-probe efficiency is given by $\epsilon = \frac{N_{MatchedProbe}}{N_{Tag}}$. In Figure 3 (b) the distribution of ΔE_{probe} is reported for the matched probe candidates corresponding to tags of Figure 3 (a) with the fit of the Gaussian part. The photon selection efficiency is measured in 8 azimuthal and two radial bins. In Figure 3 (c) the photon selection efficiency is shown for the 16 di erent bins.

The tag-and-probe method relies on the possibility to observe the positron annihilation signature just by a single photon selection, thanks to a relatively low background. In these conditions the annihilation yield can be measured also by a single photon selection by counting the events above background of the ΔE distribution or of the squared missing mass $M^2_{miss} = (p_{e^+} + p_{e^-} \quad p_\gamma)^2$ distribution which peaks to zero for annihilation photons. The di erent shapes of the two variables were used to assess systematic errors of the measurements obtained with the two-photon selection and using the $\Delta\phi$ distribution. In order to avoid double counting, the single photon based measurement consider photons within or above a middle radial position $R_{mid} = 172.83$ mm, where the two annihilation photons have the same energy.

3.1 Measurement and systematics

The acceptance, extracted from simulation, the annihilation yield and efficiency, measured in data, are combined to derive the cross-section measurement. The quantities used in the cross-

Table 1: Tag-and-probe efficiency, acceptance, total number of beam positrons collected on target and number of target electrons per unit surface.

ϵ inner ring	ϵ outer rung	A	N_{POT}	$N_{e/S}$
0.731 ± 0.009	0.714 ± 0.006	0.06424 ± 0.00025	4×10	$0.0105b^{-}$

section determination are summarized in Table 1, while the measurements obtained with di erent analysis variant are reported in 2.

Table 2: Cross-section measurement for the different analysis variant.

$\sigma(\Delta\phi)$ mb	$\sigma(\Delta E_{in})$ mb	$\sigma(M^2_{miss,\ in})$ mb	$\sigma(\Delta E_{out})$ mb	$\sigma(M^2_{miss,\ out})$ mb
1.981 ± 0.031	1.921 ± 0.028	1.889 ± 0.027	1.914 ± 0.028	1.912 ± 0.048

The measurements derived from the fit to the $\Delta\phi$, ΔE_{in} and $M^2_{miss,\ in}$ distributions can be considered equivalent, since they are based on the same reconstructed annihilation events. Therefore, the di erences will be taken into account in the assessment of the systematic uncertainty, and their average used as the cross-section measurement:

$$\sigma(e^+e^- \to \gamma\gamma) = 1.930 \pm 0.029\ (\text{stat}) \pm 0.057\ (\text{syst}) \pm 0.020\ (\text{target}) \pm 0.079\ (\text{lumi})\ \text{mb}. \quad (1)$$

The measurement is compatible with the prediction from Babayaga at NLO
$\sigma = 1.9573 \pm 0.0005\ (\text{stat}) \pm 0.0020\ (\text{syst})$ mb, where the systematic error is a conservative esti-

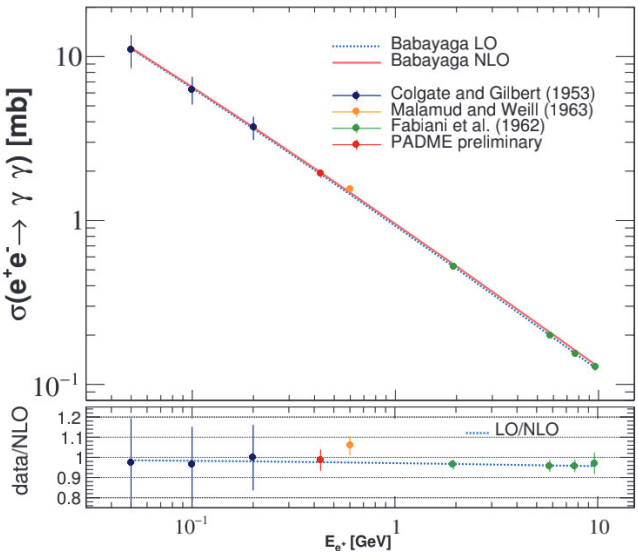

Figure 4: Two-photon annihilation cross-section vs E_{e^+} of this and previous works compared to theory predictions at LO (azure solid line) and at NLO (red solid line). On the bottom are shown the ratios between the measurements (LO) and the NLO theory predictions.

mate of the missing perturbative contributions. Figure 4 shows the agreement of the two-photon annihilation cross-section measured by PADME with the NLO theoretical predictions and with previous measurements at a similar energy scale [0], [ ], [2]. The PADME measurement is heavily relying on the data-driven efficiency measurement which exhibits a non-trivial dependence on

the azimuthal and radial sectors of ECAL. The di erence can be ascribed to local defects, non uniform distribution of background and to the shadow of the vertical dipole gap. The resulting systematic uncertainty can be estimated by looking at the di erences in the annihilation yield corrected for the efficiency obtained in the di erent azimuthal slices. The background modelling contribution can be extracted comparing the results from the fit of the $\Delta\phi$ distribution, in the two-photon selection, and of the ΔE and M^2_{miss} distributions, in the single-photon selection applied to the inner ring of ECAL. The measurements obtained in the inner and outer rings must be also considered. The two measurements are based on consistent, but experimentally di erent, definitions of the fiducial region. In addition, the contribution due to the variation of the FR radii is considered bringing a total acceptance systematics of 1.16%. A separate source of error comes from the estimate of the number of positrons on target and on the electrons number on target surface. The systematic errors combined in quadrature in the measurement of Equation 1 are summasized in table 3.

Table 3: Contribution to the systematic uncertainties of the measured annihilation cross-section.

Detector defects	Background modelling	Acceptance	Luminosity	Target atomic electron
0.020 mb	0.047 mb	0.025 mb	0.079 mb	0.020 mb

Conclusion

During Run II PADME collected $6 \times 10^{\ 2}$ POT, about half of the planned statistics, with an improved beam configuration with respect to Run I. The candle QED process $e^+e^- \to \gamma\gamma$ has been studied with 4×10 POT. The inclusive cross-section has been measured with a 5% precision. The obtained value is in agreement with QED. The uncertainty is dominated by the systematics on the evaluation of the number of POTs. The analysis shows that a compelling task is the control of the beam related background. However, the result gives confidence in a detailed understanding of the PADME key detector: ECAL. Assuming no new physics contributions, the annihilation process can be used to measure the luminosity with $\sim 3\%$ precision, enough for the search of an invisible A'.

References

1. P. Cushman, et Al., arXiv:1310.8327 (2013).
2. M. Raggi, V. Kozhuharov, Adv.High Energy Phys. 2014 (2014).
3. A.Ghigo et al., Nucl.Instrum.Meth.A 515 (2003).
4. I. Oceano , Journal of Instrumentation 15 C04045 (2020).
5. G. Piperno et al., Journal of Instrumentation, vol. 15 (2020).
6. A. Frankenthal et al., Nuclear Instruments and Methods in Physics Research, vol. 919 (2019).
7. G. Georgiev et al., RAD Association Journal, DOI:10.21175/radj.2016.03.034 (2016).
8. F.Bossi et al., arXiv:2204.05616 (2022).
9. C. M. Carloni Calame et al., Nucl. Phys. B Proc. Suppl. 131 (2004).
10. S. A. Colgate end F. C. Gilbert, Phys. Rev. 89 (1953).
11. E. Malamud, R. Weill, Il Nuovo Cimento 27 418–424 (1953).
12. F. Fabiani et al., Nuovo Cim. 25 655 (1962).